Landslide Change Characterization Experiment (*LACCE*)

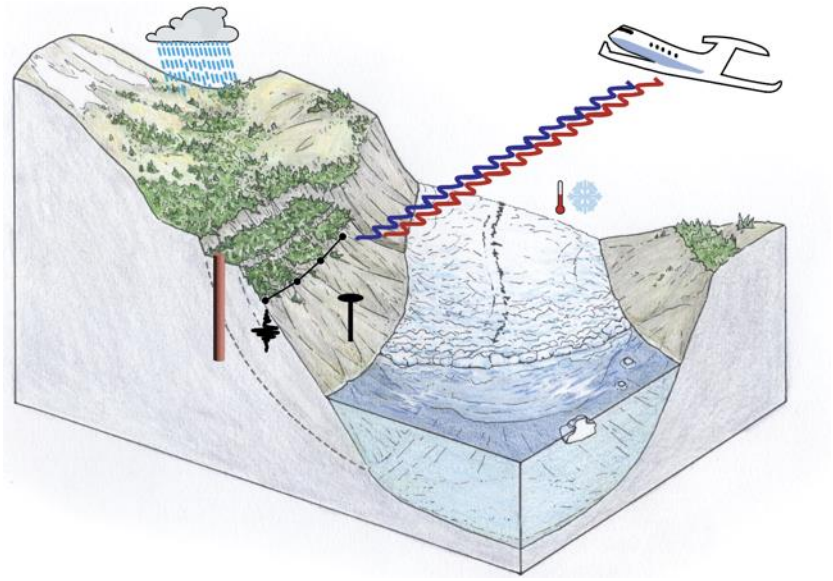

Original Image by Kim McNett and Bretwood Higman. Modified by *LACCE*. Used with permission.

White Paper for NASA Earth Venture Suborbital-4 (EVS-4)

December 8, 2025

***LACCE* PI Team:**

Alexander Handwerger (JPL, Caltech)	Principal Investigator
Noah Finnegan (UC Santa Cruz)	Deputy Principal Investigator
Seungbum Kim (JPL, Caltech)	Deputy Principal Investigator

***LACCE* Management Team:**

Thorsten Markus (NASA HQ)	Program Scientist
Shanna McClain (NASA HQ)	Program Applications Lead
Roger Chao (JPL, Caltech)	Investigation Manager

EVS-4 Management Team:

Ryan Pavlick (NASA HQ)	EVS-4 Program Scientist
Jennifer Olsen (NASA LARC)	EVS-4 Mission Manager

Jet Propulsion Laboratory, California Institute of Technology, University of California Santa Cruz, NASA Headquarters, NASA Langley Research Center.

Table of Contents

DOCUMENT CHANGE LOG

Revision	Cover Date	Sections Changed	ECR #	Reason, ECR Title, LRS #*
V0.1	Oct. 31, 2024	All	N/A	New document
V0.2	Feb. 3, 2025	All	N/A	Removed Ka-band radar from scope. Updated figures and made minor text changes.
V0.3	Apr. 15, 2025	All	N/A	Minor changes. Final Version to be released with ROSES solicitation.
V0.4	Dec. 8, 2025	Title page and schedule.	N/A	Updated project schedule and NASA personnel list.
V0.5	Jan. 12, 2026	Title page	N/A	Updated NASA personnel list.

Executive Summary

The primary goal of the *Landslide Change Characterization Experiment* (*LACCE*) is to determine the impact of precipitation extremes and glacier retreat on slope stability at a scale that has not yet been attempted. To do so, *LACCE* will answer two science questions:

1. **How do precipitation extremes (droughts and wet periods; dry regions and wet regions) impact slope stability?**
2. **How does the rapid loss of glaciers impact slope stability?**

LACCE will answer these questions using high-resolution, targeted, airborne synthetic aperture radar (SAR) data to quantify the number, size, motion, and soil moisture of active landslides, and measure their sensitivity to changes in precipitation and rapid glacier retreat. *LACCE* will focus on slow-moving landslides, which are ideal for multi-year investigations because they are relatively easy to monitor (compared to fast-moving landslides) and enable long-term observations that can be used to better constrain overall landslide mechanics, including catastrophic failure.

Science Objectives:

1. Determine the size, rate and timing of motion of active landslides across vastly different climate regimes (dry, moderate, wet; glaciated and unglaciated) at regional scales.
2. Determine landslide motion sensitivity to precipitation variability (droughts and wet periods and dry regions and wet regions).
3. Determine landslide motion sensitivity to rapid glacier retreat.

Investigation overview: Sustained airborne measurements of landslide motion and soil moisture levels, along with ground-based and laboratory data, are needed to achieve our objectives. These data will be used to develop mechanical-hydrological landslide models.

Airborne science platforms: NASA Gulfstream III or Gulfstream IV aircraft with L- and P-band radar for surface motion and soil moisture measurements.

Ground-based science platforms: Measurements of landslide motion, groundwater hydrology, and mechanical-hydrologic properties of landslide materials are needed to calibrate and validate airborne data and to develop and test landslide models. Ground instrumentation may include: (1) GPS, extensometers, and borehole inclinometers, (2) piezometers, (3) soil moisture sensors, (4) geophysical measurements (seismicity, seismic velocity and/or resistivity structure), (5) Lab experiments on landslide samples to determine frictional and hydrologic properties.

Deployment sites: To investigate the impact of changes in rainfall on landslides, we will deploy across the California Coast Ranges spanning from Los Angeles, CA to Eureka, CA. To investigate the impact of rapidly receding glaciers on landslides, we will deploy in southern Alaska around Prince William Sound.

Schedule summary: In California, deployments will be year-round at approximately monthly intervals during Years 2-4. In Alaska, deployments will be from August-October in Years 2-3. Field work to install ground instruments and collect samples will start prior to the first airborne deployments. Science team meetings will be held online at monthly intervals with annual in-person team meetings. Years 3-5 will be focused on data analysis, modeling, and dissemination.

NASA relevance: *LACCE* addresses a primary challenge in hazard forecasting and is responsive to key science questions and goals identified by the NASA Geosphere Focus Area, the Earth Surface and Interior Challenges and Opportunities for Research in ESI (CORE) Report, and the 2017 Decadal Survey as a top priority. Additionally, *LACCE* supports NASA's Earth Science to Action (ES2A) strategy, and complements and enriches other NASA efforts such as the NASA-ISRO SAR (NISAR) mission and the Observational Products for End-Users from Remote Sensing Analysis (OPERA) project.

1 Scientific/Technical Plan

Landslides are a major hazard globally that damage life, habitat, and infrastructure and also play a significant role in controlling the evolution of landscapes [1]-[3]. Each year, landslides cause more than $1 billion in damages and between 25 and 50 deaths in the US alone [4]. Globally, these numbers are many factors higher and are predicted to increase over the next century as the population expands, driving people into more remote mountainous regions [5], [6]. Notably, between 1998 and 2017 landslides killed ~18,000 people, nearly an order of magnitude more people, according to the World Health Organization, compared to ~2,400 people killed by wildfires and volcanic activity [7]. Making matters worse, landslide hazards worldwide are changing due to extreme weather in important but not well quantified ways [8]-[10].

The NASA Earth Venture Suborbital-4 *Landslide Change Characterization Experiment* (*LACCE*) investigation will bridge fundamental knowledge gaps in our ability to forecast how deep-seated landslide hazard will change in response to 1) rainfall variability and 2) glacier retreat. *LACCE* accomplishes this by using high-resolution, targeted, airborne synthetic aperture radar (SAR) data to quantify the number, size, motion, and soil moisture of active landslides and to develop mechanical-hydrological models that describe landslide deformation in response to precipitation variability and glacier retreat. The project is responsive to key science questions and goals identified by the NASA Geosphere Focus Area and the 2017 Decadal Survey as a top priority (see §1.1.2 and §1.2). *LACCE* will focus on detecting and monitoring large (> 300 m long), deep-seated (> 2 m deep), slow-moving (rates < 100 m/yr) landslides. Slow-moving landslides, as defined here, are bodies of soil and rock that move by frictional sliding along discrete surfaces at rates ranging from a few mm/yr to 100 m/yr [11]. Occasionally, slow-moving landslides can accelerate rapidly and fail catastrophically, providing an opportunity to test models that attempt to understand this process transition [12]-[15]. In addition, slow-moving landslides are key natural laboratories for multi-year investigations because they are relatively easy to monitor (especially compared to fast-moving landslides) and enable long-term observations that can be used to better constrain overall landslide mechanisms, including catastrophic failure (e.g., [16]).

LACCE will not investigate the role of wildfire on landslides, nor will it investigate mass wasting processes associated with single event triggers such as rainfall-triggered debris flows, volcanic lahars, and shallow surficial processes such as slumps or rockfalls because the processes that nucleate these types of mass wasting events are typically very transient in nature and lack measurable pre-event motion observable with airborne systems. While there is undoubtedly a strong relationship between extreme weather, wildfires, and landslides (e.g., [17]), these types of mass movements are typically relatively small, initiate in seconds and travel at high rates (m/s), making their motion unobservable with airborne systems.

1.1 *LACCE* Science Goals and Objectives

LACCE will characterize changes in slope stability at a scale that has not yet been attempted. To do so, *LACCE* will achieve the following Science Objectives:

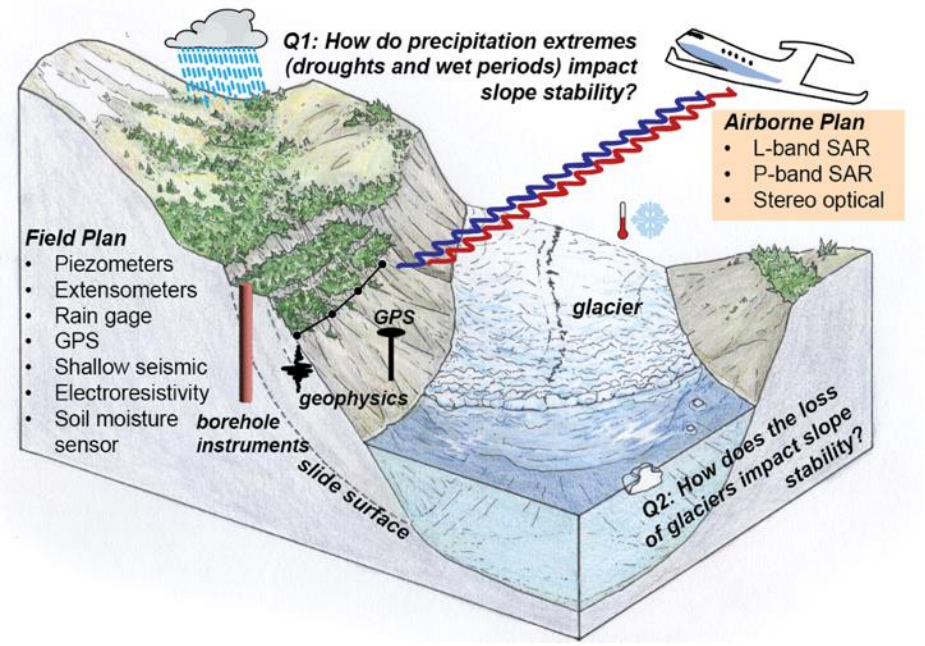

Fig. 1. Schematic cross section of a landslide showing airborne plan, field plan, and key research questions addressed by *LACCE*. Note drawing is designed for Alaska study site but airborne/ground-based plans are relevant to California. Original Image by Kim McNett and Bretwood Higman. Modified by *LACCE*. Used with permission.

Objective 1 (O1): Determine the size, rate and timing of motion of active landslides across different precipitation regimes (dry, moderate, wet). *LACCE* answers: What is the number, size, and behavior of unstable hillslopes at regional-scales? (see Question 1 in § 1.1.3)

Objective 2 (O2): Determine landslide motion sensitivity to precipitation variability. *LACCE* answers: How do precipitation extremes (droughts and wet periods and dry regions and wet regions) impact slope stability? (see Question 1 in § 1.1.3)

Objective 3 (O3): Determine the size, rate and timing of motion of active landslides in deglaciating areas. *LACCE* answers: What is the number, size, and behavior of unstable hillslopes at regional-scales? (see Question 2 in § 1.1.3)

Objective 4 (O4): Determine landslide motion sensitivity to rapid glacier retreat. *LACCE* answers: How does the loss of glaciers impact slope stability? (see Question 2 in § 1.1.3)

1.1.1 Compelling Nature of the Investigation

Precipitation patterns vary regionally, which can impact landslide hazards in different ways [8]-[10]. First, shifting precipitation patterns are causing extreme wet periods to become more common in some places [18], leading to more frequent periods where pore-water pressures drive hillslopes to a critical state [9], [11]. At the same time, rapid glacier retreat, which is removing

support near landslides' lowermost boundary - a process known as "debuttressing" - along some of the steepest hillslopes on the planet [19], [20]. This loss of slope support can shift the balance of a hillslope to failure, triggering landslides during and after glacial retreat [21], [22]. Furthermore, many of these retreating glaciers are in deep fjords, which means that if slopes collapse, they could trigger local tsunamis that are a major secondary hazard. Yet, assessing future landslide behaviors is difficult due to uncertainties in both our understanding of how rainfall variability and ice loss translate into slope stability. ***LACCE* will characterize changes in landslide behavior in response to these two different variables (rainfall variability in space and time, glacier retreat) to improve forecasting of deep-seated landslide hazards.**

Precipitation changes and their impact on landslides are not fully understood. In western California (CA), which has a Mediterranean climate with cool wet winters and dry summers, rainfall is the key driver of landslides annually, particularly within mechanically weak, clay-rich sedimentary rocks in the Coast Ranges (e.g., [23], [24]). Models predict changes in the

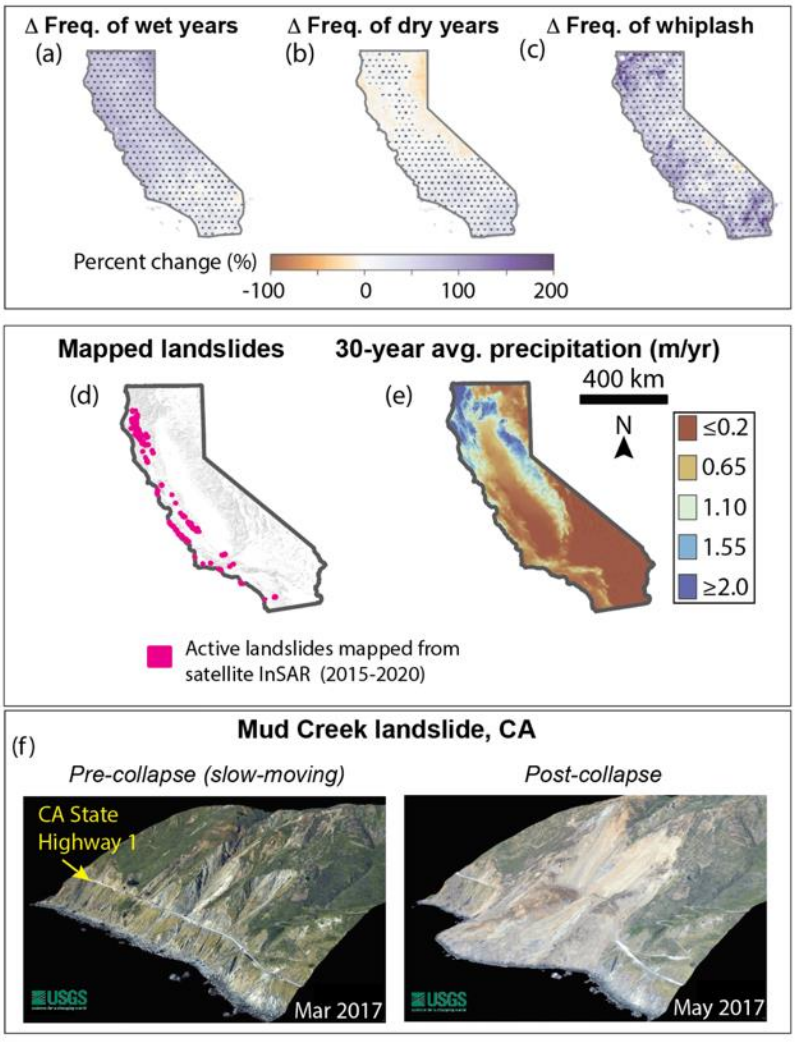

Fig. 2. *LACCE* will address how changes in precipitation in space and time impact landslides. Predicted change in (a) frequency of wet years, (b) dry years, (c) year-to-year whiplash (wet years followed by dry years or vice versa) occurrence. Values shown are for percent changes between historical (1950–2005) mean and late-century (2044–2099) mean conditions relative to historical period. (a-c) Modified from [25]. (d) Location of study area showing active landslides identified with previous satellite InSAR (interferometric synthetic aperture radar) analyses between 2015-2020 [23]. (e) 30-year (1990-2019) mean precipitation (m/yr). (f) Imagery of Mud Creek landslide; a slow-moving landslide that collapsed in 2017 due to extreme rainfall after > 8 years of slow-motion [26].

distribution (rather than total amount) of rainfall over the next century [18], [25], [27]. In particular, models predict that short, intense winter rain periods (analogous to the 2022-2023

winter) will increase (Fig. 2). At the same time, droughts are also predicted to become more frequent, leading to a 25-100% increase in extreme dry-to-wet precipitation transitions - so called "whiplash" events [18]. Recent work has shown that landslide size, particularly thickness, governs response to year-to-year rainfall changes [28], [29]. Landslides speed up and slow down during wet and dry years, with some landslides remaining stationary during dry years and then reactivating during wet years [23], [24], [30]. Some landslides completely change behaviors and transition from slow-to-fast motion in response to extreme rainfall [12], [15], [26]. For example, the Mud Creek landslide in Big Sur, CA collapsed after more than 8 years of slow motion during the extreme rainfall of 2017 (Fig. 2f). Because CA has a steep precipitation gradient from north to south (Fig. 2e), it can be used to explore landslide response for places that are becoming wetter or drier on average. Yet, we currently lack the ability to predict these behaviors and generally have poor constraints on the kinematic behavior of landslides and groundwater conditions that control their motion. *LACCE* will develop a well-constrained understanding of landslide sensitivity to precipitation variability and is thus crucial to landslide hazard forecasting and mitigation, not only in CA, but in similar climates worldwide (e.g., parts of southern Europe, New Zealand, Japan, and Peru, to name a few).

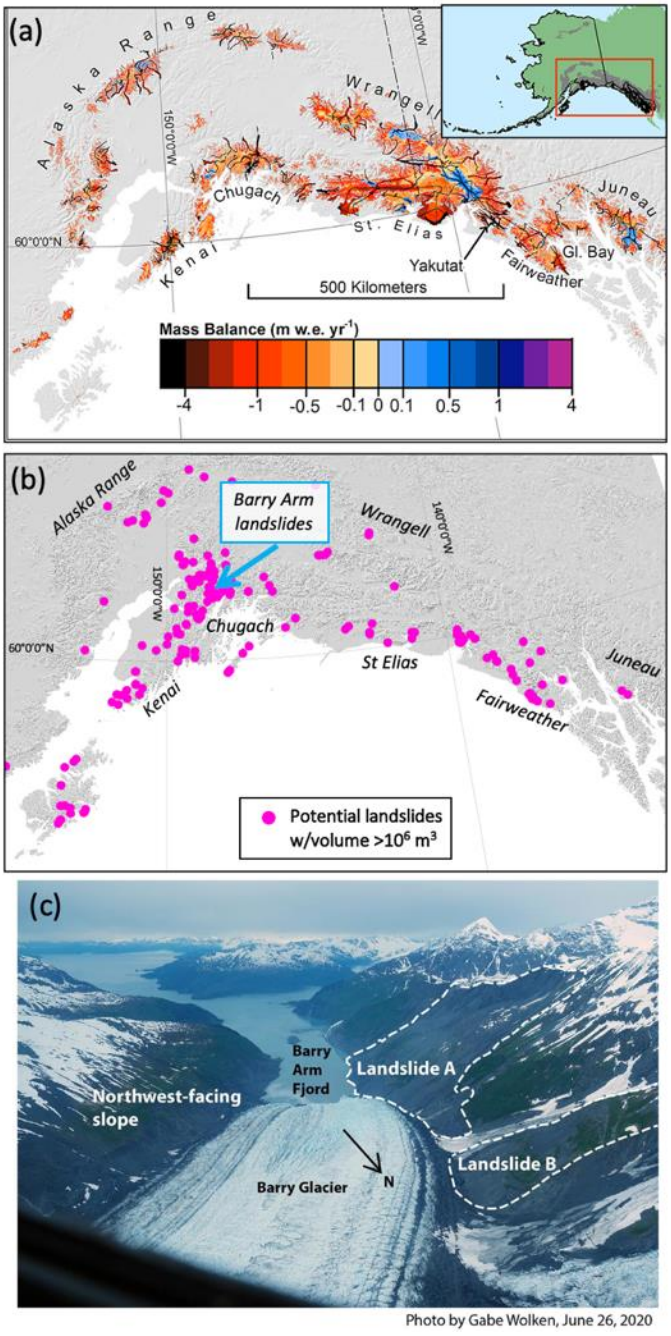

Fig. 3. *LACCE* will address the lack of kinematic observations at Alaskan landslides. (a) Changes to glacier mass balance between 1994 and 2013 measured from NASA's Operation IceBridge airborne altimetry. Mass balance change is shown in meters of meltwater equivalent per year. Red-to-black colors show where glaciers have thinned, and blue-to-purple colors are where they have thickened. Modified from [31]. (b) Potential large landslides identified from topographic data and optical images. Almost none of the landslides shown (b) have kinematic measurements. Our investigation will determine the total number of active landslides in this region and quantify their rates. (c) Aerial photo of Barry Arm landslides and Barry glacier.

Rapid glacier loss and its impact on landslides are not well understood. Southeastern Alaska (AK) has a maritime climate with many large glaciers at low elevations that are retreating rapidly past steep slopes (Fig. 3) [31], [32]. Over the next century further glacier retreat is likely [33]. This rapid glacier retreat is causing large reductions in rockslope shear strength due to debuttressing, with increasing landslide occurrence and susceptibility [21], [34] to an extent that is not well quantified. Preliminary investigation [34] has shown that ~100 landslides with volumes in the 10s or 100s of millions of cubic meters have initiated on heavily fractured, deglaciating slopes in this region across a wide range of rock types, and more landslides are expected to occur with continued ice loss. Recent studies in this region [35], [36] used satellite-based interferometric synthetic aperture radar (InSAR) to show that at least 43 of these landslides are active and 11 are potentially tsunamigenic. This work, however, also emphasizes the challenges of monitoring the steep, often snow-covered fjords in AK with satellite data. One of these landslides in Barry Arm, Prince William Sound (Fig. 3c), has received considerable attention in recent years by researchers [21], the state of AK, and the U.S. Geological Survey [37], due its size, location, activity state, and tsunami potential. While the landslide has slowed recently, it is unstable and is at risk of collapsing. For many of the other landslides, there is only circumstantial evidence that these instabilities are becoming more active and/or pose increasing hazards. Importantly, however, several large landslides in this region have failed catastrophically in the past and triggered devastating tsunamis with wave heights >150 m: e.g., several landslides in Lituya Bay [38], the 1967 Grewingk Lake landslide [39], and the 2015 Taan landslide [40]. The risk to humans and infrastructure presented by landslide-generated tsunamis is likely growing as slopes lose glacier buttressing, increasingly large water bodies become exposed, permafrost in some of these slopes weakens or thaws [10], and tourist travel to the region increases. The largest US commercial fisheries depend on ports located on steep mountainous coastlines near rapidly receding glaciers. In 2018, 1,169,000 tourists traveled AK's glacier-carved coastlines by cruise ship [41], each with a passenger capacity of up to 5,000 people. A landslide-generated tsunami could therefore create one of the largest natural disaster fatalities in the US in a century. This emerging hazard is by no means restricted to AK, though it is likely most acute there. Other glacier-carved coastal landscapes in Greenland, Iceland, Chile, Norway, and Canada are similarly vulnerable (e.g., [22], [42], [43]). Thus, it is essential we identify and monitor active landslide slopes in this region in order to constrain the mechanisms that control and predict their behavior.

Although previous studies have begun to unravel some of the relationships between landslides, precipitation, and glacier extent changes (e.g., [9], [10], [28], [29], [44], [45]), there continue to be many unknowns that prevent us from fully understanding these evolving landslide hazards. Some of the main limitations of prior studies are that the total number of landslides moving at any given time is not well quantified, nor are the groundwater conditions. Satellite-based measurements, such as those from InSAR or pixel tracking of optical and radar images, have revealed large numbers of active landslides that were previously unknown or undocumented [29], [35], [46], [47]. Yet these satellite-based inventories are limited due to moderate-to-coarse spatial resolutions, which results in a lack of information on the smallest and potentially most dynamic landslides, and from observational biases that cannot image slopes in steep landscapes or landslides moving in certain directions (resulting from predetermined satellite flight paths and look angles). Furthermore, measurements of groundwater are typically limited to point-based locations within single landslides which lack the high resolution spatial and temporal coverage needed to characterize the groundwater system. **Airborne instruments are the only means of providing sufficiently high spatial and temporal coverage over large regions to reveal complete active landslide**

inventories and quantify their motion. This information will allow us to explore how landslides are responding to changing environmental conditions.

1.1.2 Value to Advancing NASA's Earth Science Objectives

The value of our investigation to advance NASA's Earth science objectives is presented in §1.2.

1.1.3 Driving Science Questions and Hypotheses

Changes in precipitation and glacier extent are expected and are already measurable. Landslide sensitivity, i.e., velocity response, to these changes depends on the landslide size and geography in predictable ways. *LACCE* addresses two questions (Q) related to these changes and tests hypotheses (H) related to each:

- **Q1**: How do precipitation extremes (droughts and wet periods; dry regions and wet regions) impact slope stability?
    - **H_{Q1a}**: Large landslides are less sensitive to interannual rainfall variability compared to small landslides. Thus, changes in shorter-term (decadal scale or less) landslide hazards will be accommodated by smaller and more dynamic landslides.
    - **H_{Q1b}**: The driest regions, where precipitation rates are generally less than the rates at which water drains from hillslopes, will experience the largest changes in landslide activity.
- **Q2**: How does the loss of glaciers impact slope stability?
    - **H_{Q2a}**: Loss of glacier buttressing is a major stress event for slopes leading to a peak in failure probability as an ice-face retreats beneath a slope.
    - **H_{Q2b}**: Landslides move faster near the glacier calving front where the rate of stress change is highest.

1.1.4 How Science Questions and Hypotheses Will Be Addressed

Impacts of changing precipitation

To test H_{Q1a} and H_{Q1b}, *LACCE* established science objectives O1 and O2, which involve inventorying and tracking landslide 3D surface motion and 3D geometry with airborne SAR (Fig. 4) during wet-to-dry years and in wet-to-dry hydroclimates in CA (Fig. 2). The ideal airborne system for *LACCE* is the NASA Gulfstream III or Gulfstream IV aircraft with L- and P-band radar for surface motion and soil moisture measurements. Additionally, stereo optical imagery may be useful for topographic change measurements. The rationale for O1 is to determine the location, extent, size, and displacement rate of moving landslides. For each region, landslides are imaged by 3 to 4 overlapping flight paths from different acquisition geometries, allowing for measurements of true 3D surface velocity. These 3D surface velocity measurements are needed to infer the actively deforming thickness, volume, and frictional strength of each landslide [48]. Measurements of the shape and depth of the landslide failure surface are critical for understanding landslide behavior [48], [49]. However, constraints on subsurface geometry are lacking because these types of landslides rarely fully evacuate material to create measurable hillslope scars. Fig 4.

shows an example of our approach for the Mud Creek landslide. 3D InSAR was used to measure surface velocity and estimate the pre-collapse thickness and volume. Comparison with pre- and post-collapse topographic data from lidar shows we can constrain the landslide volume within the same order of magnitude, even prior to the landslide collapse, thereby providing us with important data needed to assess landslide hazards.

With this information, *LACCE* will accomplish O2, which involves measuring the sensitivity of landslides to precipitation, and thus groundwater storage variability at the CA sites. Specifically, *LACCE* seeks to measure the impact of year-to-year changes in landslide hydrology (e.g., soil moisture, pore-water pressure) on landslide kinematics as a function of landslide size and hydroclimate (Figs. 5 and 6) allowing us to test H_{Q1a}-H_{Q1b}. *LACCE* will acquire high resolution, spatially continuous measurements of soil moisture using airborne radar data for all landslide slopes, acquired with two frequencies (L-band and P-band) and with 4 polarizations (Fig. 5). In addition, soil moisture time series maps will be produced using backscatter coefficients (e.g., [50]). The near-surface soil moisture measurements provide key boundary conditions that are applied to groundwater hydrology models, such as the variably unsaturated groundwater flow models *vs2dt* and *Hydrus 3D* [51], [52], [53], that enable us to produce accurate pore-water pressure calculations at depth (e.g., [30]).

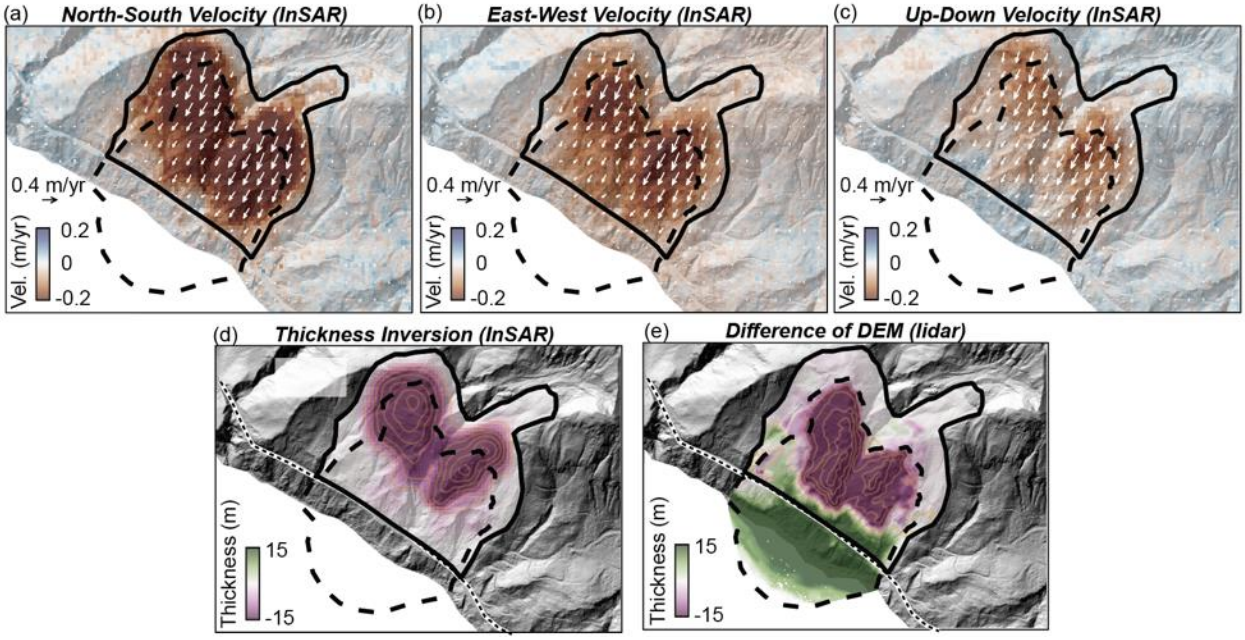

Fig. 4. *LACCE* will use 3D surface velocity measurements to invert for the subsurface geometry and volume of active landslides. Example dataset for Mud Creek landslide, CA. (a-c) North-South (red = south), East-West (red = west), Up-Down (red = down) velocity, respectively, with velocity vectors (white arrows) draped over a shaded relief map. (a-c) Modified from [12]. (d) Preliminary landslide thickness inversion map from 3D InSAR and volume conservation. Orange lines show 5 m thickness contours. (e) Vertical distance change using from pre- (2016) and post-collapse (2018) lidar point cloud. Orange lines show 10 m contours. Positive values correspond to material deposit after failure. Solid black line shows pre-collapse landslide boundary. Dashed line shows a post-collapse scar boundary.

Ground-based measurements of surface motion and groundwater hydrology at four landslides in wet, moderate, and dry hydroclimates will be used to calibrate and validate airborne data. Ground-based instrumentation may include: (1) borehole piezometers, extensometers, and inclinometers to measure pore-water pressure and motion at depth (e.g., [24], [30], [54]), (2) soil moisture sensors (e.g., [50]), (3) geophysical measurements such as electrical resistivity (e.g., [24]) and shallow seismic velocity measurements (e.g., [55]) for groundwater and subsurface geometry. Characterization of hydrological parameters of landslide material in the field (e.g., slug tests for hydraulic conductivity) and in the laboratory is also necessary. In addition, laboratory measurements (biaxial and/or triaxial shear, or ring-shear) on landslide samples are needed to determine frictional strength (friction angle, rate-dependent properties) needed to develop landslide models, such as a 3D method of columns limit-equilibrium model (e.g., [56]), critical state model (e.g., [57]) and rate and state friction model for landslides (e.g., [58], [59], [60]). These models will allow us to better understand the mechanisms controlling the landslide dynamics and to make model forecasts. Figure 5 shows a conceptual workflow for how to combine airborne radar data, ground data, and models to forecast landslide motion.

The landslide sensitivity to precipitation variability can be quantified via a characteristic filling timescale (t_f) or, equivalently, the residence time of water within a landslide, $t_f = hs_{yu}/(p\text{-}d)$, where h is landslide depth, s_{yu} is the ultimate specific yield, the difference between porosity and residual moisture content, p is precipitation rate, and d is drainage rate. For most landslides, failure potential is proportional to the depth of water within a landslide relative to the overall depth of the landslide [61]. Hence, changes in failure potential should occur more rapidly in smaller landslides compared to larger landslides. For example, for typical values of slow-moving landslides occurring within the clay-rich rocks in CA (e.g., [30]), s_{yu}= 0.2, d = 0.003 m/day, and p = 0.05 m/day, a 5 m deep landslide would fill after 20 days of rainfall (assuming it started with no water), whereas a 40 m deep landslide would require 170 days of rainfall to fill (assuming it started with no water), which is exceedingly unlikely in CA's climate which has a rainy season from October to May each year. In the absence of rainfall, a 5 m deep landslide would require about 1 year to drain, whereas a 40 m deep landslide would require about 7 years of drought to drain, again something beyond what is typically observed in CA's droughts [18]. These calculations help explain why smaller, shallower landslides are more sensitive to interannual rainfall variability than larger, deeper landslides [28], [29]. Thus H_{Q1a}, will be addressed by quantifying landslide response as a function of landslide size to determine if smaller landslides (1-5 m deep) show an increase in activity due to increases in rainfall intensity over short timescales (days to weeks long) [18], [27].

Following on this, H_{Q1b} will be addressed by quantifying the landslide sensitivity across a large wet-to-dry rainfall gradient in CA (Figs. 2 and 6). **This wet-to-dry gradient can serve as a proxy to understand landslide response for places that are becoming wetter or drier on average**. Using the same framework described above, we expect that differences in the precipitation rate will lead to detectable changes in landslide behavior across rainfall gradients. Currently, the typical winter rainfall rate is ~8-10 mm/day in the wettest landslide areas, 4-7 mm/day in moderate areas, and 2-4 mm/day in dry areas (Fig. 2e). Whereas landslide drainage rates are comparable to winter rainfall rates in the dry regions of the study area, rain rates are far in excess of drainage rates in the wet part of the state. This comparison suggests that negative deviations from the climatological precipitation norms should have a disproportionate impact on landslide displacement rates in the drier part of the study region, where drainage rates and precipitation rates are comparable, and storage is therefore much more sensitive to precipitation variability.

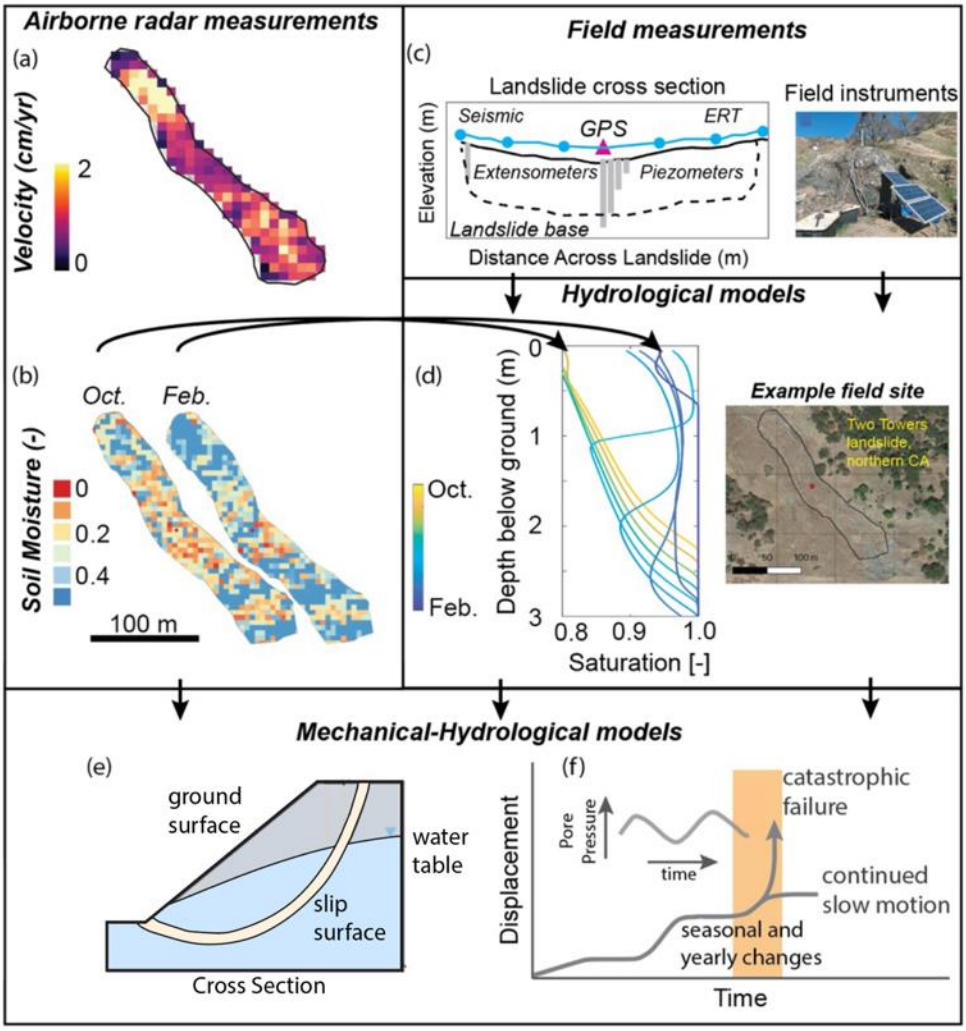

Fig. 5. *LACCE* will provide the first ever regional-scale high resolution soil moisture and velocity measurement that can be used for landslide models. Example (a) velocity and (b) Soil moisture maps for the Two Towers landslide, northern CA retrieved using airborne SAR images. Soil moisture map from [50] and velocity map from [29]. (c) Schematic landslide cross section showing ground-based instrument plan. (d) Modeled profiles of subsurface saturation modified from [30]. (e-f) Schematic model working concept. (f) Modified from [11].

In addition to the airborne and ground-based data acquired by *LACCE*, the *LACCE* team will also process and analyze relevant, freely available satellite imagery to identify and monitor landslides (e.g., NISAR, Sentinel-1, Sentinel-2, and commercial SAR and optical datasets available through NASA's Commercial Satellite Data Acquisition program).

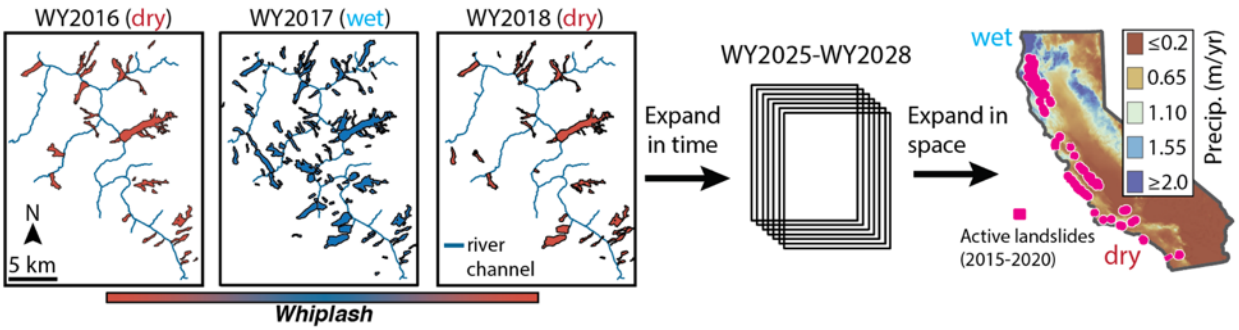

Fig. 6. *LACEE* will inventory and monitor active landslides in different hydroclimates during droughts and wet periods. Example landslide inventory for a subsection of a wet region (Eel River catchment), northern CA from [29]. Maps show large changes in landslide activity (polygons) due to year-to-year variations in rainfall (i.e., whiplash) occurring in the smallest landslides. WY2016 and WY2018 were both dry years and WY2017 was extremely wet. Landslide inventories in (a-c) were made with airborne InSAR. WY = water year, which is the time period from Oct. 1 to Sep 30.

Impacts of rapid glacier retreat

To illuminate impacts of rapid deglaciation on landslide failure, *LACCE* will test H_{Q2a} and H_{Q2b}, and establish O3 and O4, which involves inventorying and tracking 3D surface motion and 3D geometry of landslides in areas that are under rapid deglaciation in the fjords of southeast AK (Figs. 3 and 7). Some of the glaciers in this region are retreating at rates of km/yr which allow us to examine hillslope response within the study period. As mentioned above, the rationale for O3 is to determine the location, size, and rate of slow-moving landslides. Similar to the CA sites, this requires measuring 3D surface velocity from airborne SAR and applying volume conservation to infer the actively deforming thickness, volume, and frictional strength of each landslide (e.g., Fig. 4). In addition, ground-based measurements of surface motion and groundwater hydrology at two selected landslides will be used to calibrate and validate airborne data. Importantly, *LACCE* will provide the first high resolution regional map of active landslide motion in the AK fjords where satellite data has limited use. Within the set of active landslides identified, the *LACCE* team can constrain the volume of actively deforming slow landslides in order to highlight those landslides whose size and local bathymetric conditions pose an acute risk of tsunamigenesis. While there is a likely relationship between rapid glacial thinning and slope failure, as is evidenced from individual case studies that show that the loss of glacier support at the base of steep slopes increases landslide hazard, many fundamental questions about this process are not understood. Chief among these uncertainties is the extent to which the stress perturbation induced by ice retreat is important, compared to the stress perturbations related to other landslide driving factors such as rainfall. For example, because of the relatively small stresses involved in ice buttressing, some have challenged or deemphasized [62] the role of ice buttressing in strengthening rock slopes. By accomplishing O3 and O4 and testing H_{Q2a} and H_{Q2b}, *LACCE* will provide key information that sheds light on this controversial topic by demonstrating whether landslide failures are localized near rapidly retreating ice fronts or whether they follow the contours of the much broader regional precipitation gradients.

In addition to the airborne and ground-based data acquired by *LACCE*, all freely available satellite SAR and optical data useful for identifying and monitoring landslides will be processed and analyzed (same as for the CA sites).

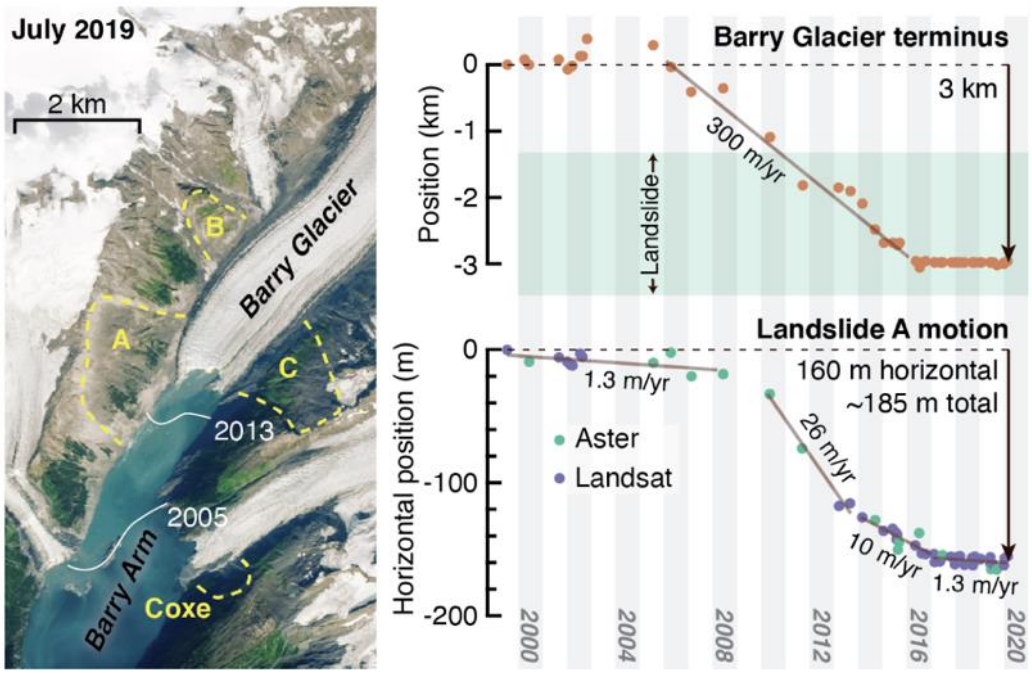

Fig. 7. *LACCE* will quantify the displacement rate and geometry of landslides in AK. Example figure showing horizontal displacement of the Barry Arm landslide and its correlation with the Barry Glacier calving front retreat. (lower right) The cumulative magnitude of horizontal displacement constrained from satellite imagery between 1999 and 2020. (upper right) The Barry Glacier calving front position time series. The shading denotes the landslide position along the glacier centerline. Modified from [21].

1.1.5 Need for Sustained Airborne Measurements

Sustained airborne measurements of landslide motion are needed to achieve our Investigation Objectives and to test our hypotheses. Additional airborne measurements of topography may benefit the investigation. Landslide motion varies over both seasonal and interannual time scales due to external factors. For CA, we need sustained measurements during Years 2-4 from L-band radar 12x per year (Baseline) or 9x per year (Threshold) in wet, moderate, and dry hydroclimates. A single data acquisition flight for CA would take ~12 hours (or two 6-hour flights per month). We need P-band at a similar cadence, however due to a large P-band exclusion zone in CA, the spatial coverage would be greatly reduced, and the approximate flight time is 6-8 hours. For AK, we need measurements, 2x per year (Baseline) for Years 2-3 (4 total) or 1x per year for Years 2-3 (2 total) during snow-free periods (August-October). A single data acquisition flight for AK would take 6 hours. The reduced frequency of the AK sites is appropriate because the timescale of glacier retreat is over annual rather than seasonal scales. Sustained measurements of ground surface topography (Baseline) may provide additional information to better understand landslides.

1.1.6 Allocation of Functional and Performance Characteristics

The established Investigation Science Objectives (c.f. §1.1, §1.1.4) allow us to derive the baseline and threshold investigation Science Requirements (see § 1.3). Furthermore, our baseline and threshold Science Objectives are allocated to Measurements and Modeling Requirements (see §A1.1.1, §A1.1.2.), as well as other investigation Functional Requirements as described in our Science Observational Profile (§1.4.1).

1.2 Relevance to Earth Science

Table 1.2-1: Relevance to Earth Science and the 2017 Decadal Survey.

2017 DS Recommendations	ESD Focus Area/Goal	Investigation's Science Question Addressed
S-1c. Forecast and monitor landslides, especially those near population centers. Science Importance: Very important	**ESD Focus Area**: Geosphere: Dynamics And Hazards. **Societal or Science Question/Goal: S1**. How can large-scale geological hazards be accurately forecast in a socially relevant time frame?	Science Question Q1-Q2 address.
H-4a. Monitor and understand hazard response in rugged terrain and land margins to heavy rainfall, temperature, and evaporation extremes, and strong winds at multiple temporal and spatial scales. Science Importance: Very important	**ESD Focus Area**: Global Hydrological Cycles and Water Resources Panel. **Societal or Science Question/Goal: H-4**. How does the water cycle interact with other Earth system processes to change the predictability and impacts of hazardous events and hazard chains (e.g., floods, wildfires, landslides, coastal loss, subsidence, droughts, human health, and ecosystem health), and how do we improve preparedness and mitigation of water-related extreme events?	Science Question Q1 partially address.

The *LACCE* investigation directly addresses 2017 Decadal Survey priorities established by the Earth Surface and Interior: Dynamics and Hazards Panel. These priorities are described by Societal and Science Question Goals (S-1) "How can large-scale geological hazards be accurately forecast in a socially relevant time frame?" and (S-4) "What processes and interactions determine the rates of landscape change?" As well as those made by the Global Hydrological Cycles And Water Resources Panel, including (H-4) "How does the water cycle interact with other Earth system processes to change the predictability and impacts of hazardous events and hazard chains (e.g., floods, wildfires, landslides, coastal loss, subsidence, droughts, human health, and ecosystem health), and how do we improve preparedness and mitigation of water-related extreme events?". The *LACCE* investigation aligns with the ESD Geosphere focus area and its goal to "support research and analysis of solid-Earth processes and properties from crust to core". Furthermore, we also address recommendations of NASA's 2016 Challenges and Opportunities for Research in ESI (CORE) Report aimed at challenges "1) what is the nature of deformation associated with plate boundaries and what are the implications for …other related natural hazards "and "2) how do tectonic processes and climate variability interact to shape the Earth's surface and create natural hazards" Lastly, the *LACCE* investigation complements other NASA strategies/investigations/missions/projects such as Earth to Action, NISAR mission and the OPERA project.

1.3 Baseline and Threshold Science Requirements

LACCE's Baseline Investigation fulfills all the Science Objectives (c.f. §1.1, §1.1.4). Our investigation requirements drive our Measurement, Model, and other Functional Requirements (see §A1.1.1, §A1.1.2, §1.4.1.)

Baseline Requirements (Objectives 1-4):

B(a). Measure 3D displacement 12x per year in Years 2-4 (36 total) in CA and 2x per year in Years 2 & 3 (4 total) in AK with L-band and P-band airborne SAR campaigns.

B(b). Measure soil moisture 12x per year (36 total) in CA and 2x per year in Years 2-3 (4 total) in AK with L-band and P-band airborne SAR campaigns.

B(c). Measure surface topography with airborne stereo optical imagery if co-flying with airborne SAR (see B(a)).

B(d). Measure 3D displacement with ground-based GPS and soil moisture with ground-based soil moisture sensors continuously at four sites in CA and two sites in AK for 3 years.

B(e). Apply volume conservation approach to invert for subsurface landslide geometry using 3D surface motion measurements (see B(a)).

B(f). Measure landslide thickness with borehole extensometers, pore-water pressure with borehole piezometers, and rainfall with rain gauges continuously at four sites in CA.

B(g). Measure subsurface landslide structures and groundwater using seismic velocity and electroresistivity 4x per year (12 total) at four selected sites in CA and 1x per year (3 total) in AK.

B(h). Measure frictional strength of landslide material using triaxial and/or ring-shear apparatus laboratory experiments once during the project period.

B(i). Model landslide pore-water pressures using groundwater models and model landslide motion using mechanical-hydrological models, such as rate-and-state friction and/or 3D method of slices based on inputs from laboratory, ground-based, and remote sensing measurements.

Threshold Requirements (Objectives 1-3):

T(a). Measure 3D displacement 9x per year in Years 2-4 (27 total) in CA and 1x per year in Years 2 & 3 (2 total) in AK with L-band and P-band airborne SAR campaigns.

T(b). Measure soil moisture 9x per year (27 total) in CA and 1x per year in Years 2 & 3 (2 total) in AK with L-band and P-band airborne SAR campaigns.

T(c). Measure 3D displacement with ground-based GPS and soil moisture with ground-based soil moisture sensors continuously at four sites in CA and one site in AK for 3 years.

T(d). Apply volume conservation approach to invert for subsurface landslide geometry using 3D surface motion measurements (see T(a)).

T(e). Measure landslide thickness with borehole extensometers, pore-water pressure with borehole piezometers, and rainfall with rain gauges continuously at four sites in CA.

T(f). Measure frictional strength of landslide material using triaxial and/or ring-shear apparatus laboratory experiments once during the project period.

T(g). Model landslide pore-water pressures using groundwater models and model landslide motion using mechanical-hydrological models, such as rate-and-state friction and/or 3D method of slices based on inputs from laboratory, ground-based, and remote sensing measurements.

1.4 Science Implementation

1.4.1 Science Observing Profile

Based on our Science Objectives, *LACCE* has identified the following Science Investigation Functional Requirements (operational requirements) to meet our observation requirements in Table 1.4.1-1. To meet our Investigation Functional Requirements, *LACCE* will implement the following flight plans and ground campaigns shown in Table 1.4.1-2 and in Figure 8. Ideal airborne systems include NASA Gulfstream III or Gulfstream IV aircraft with L-band and P -band radar. Ground-based instruments will be deployed for continuous measurements and during campaign surveys (Fig. 8). Data will be analyzed as soon as it is available from the instrument providers. Key milestones include airborne and ground deployments, investigation reviews, and dissemination of results at annual American Geophysical Union and European Geosciences Union conferences/town halls and in multiple peer-reviewed publications.

Table 1.4.1-1. Investigation Functional Requirements. Airborne measurements in blue text, ground measurements in green text.

Science Question & Objective Addressed	Threshold (T) or Baseline (B)	Investigation Functional Requirements
[Q1 -> O1], [Q1 -> O2], [Q2 -> O3], [Q2 -> O4]	**B**	**Airborne Campaign (Example flight plans shown in Fig. 8):** • Acquire airborne data in CA (imaged area ~ 30,000 km^2) with radar (L-, P-band) and co-flying stereo optical to measure 3D ground surface displacement, ground surface elevation, soil moisture. • Acquire airborne data in AK (imaged area ~ 25,000 km^2) with radar (L-, P-band) and co-flying stereo optical for 3D ground surface displacement and ground surface elevation. **Temporal frequency:** 12x per year for CA in Years 2-4. 2x in Years 2 & 3 for AK. **Ground Campaign:** • Sample four landslide sites (see Fig. 8) in CA with 1) GPS (1 to 2 per site, 4 or 8 total) and extensometers to measure 3D ground surface motion, 2) borehole inclinometers (1 to 3 per site, 4 to 12 total) to measure subsurface geometry, 3) soil moisture sensors (1 to 3 per site, 4 to 12 total) to measure soil moisture, 4) borehole piezometers (1 to 3 per site, 4 to 12 total) to measure pore-water pressure, 5) rain gauges (1 per site, 4 total) to measure precipitation, 6) seismic geophones (50 per campaign, 50 total) and electroresistivity (50 per campaign, 50 total) meters to measure subsurface structure and water content, 7) sample material (1 per site, 4 total) to measure landslide material strength and hydraulic properties. • Sample three landslide sites (see Fig. 8) in AK with 1) GPS (1 to 2 per site, 2 or 4 total) and extensometers to measure 3D ground surface motion, 2) seismic geophones (50 per campaign, 50 total) and electroresistivity (50 per campaign, 50 total) meters to measure subsurface structure and water content, 3) soil moisture sensors (1 to 3 per site, 2 to 6 total) to measure soil moisture, 4) sample material (1 per site, 2 total) to measure landslide material strength and hydraulic properties. **Temporal frequency:** Field campaigns 1-2x per year in CA and 1x in year in AK. GPS, borehole measurements are continuous after deployment. Seismic and electroresistivity are campaign based. Landslide strength and hydraulic measurements are performed once during study.

[Q1 -> O1], [Q1 -> O2], [Q2 -> O3],	**T**	For Threshold we reduce the number of deployments per year and measurement types (see §1.3).

Table 1.4.1-2. Operational milestones (Baseline).

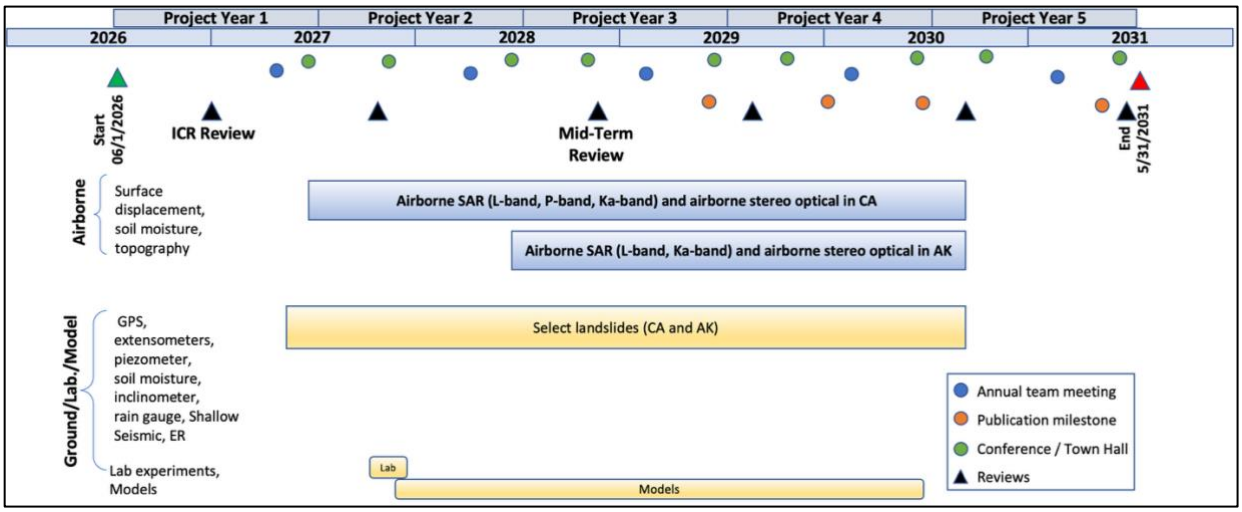

1.4.1.1 Identification as a Small Investigation

LACCE was selected as a Small Investigation focused primarily on how precipitation changes impact landslides and secondarily on how rapid glacier retreat impacts landslides.

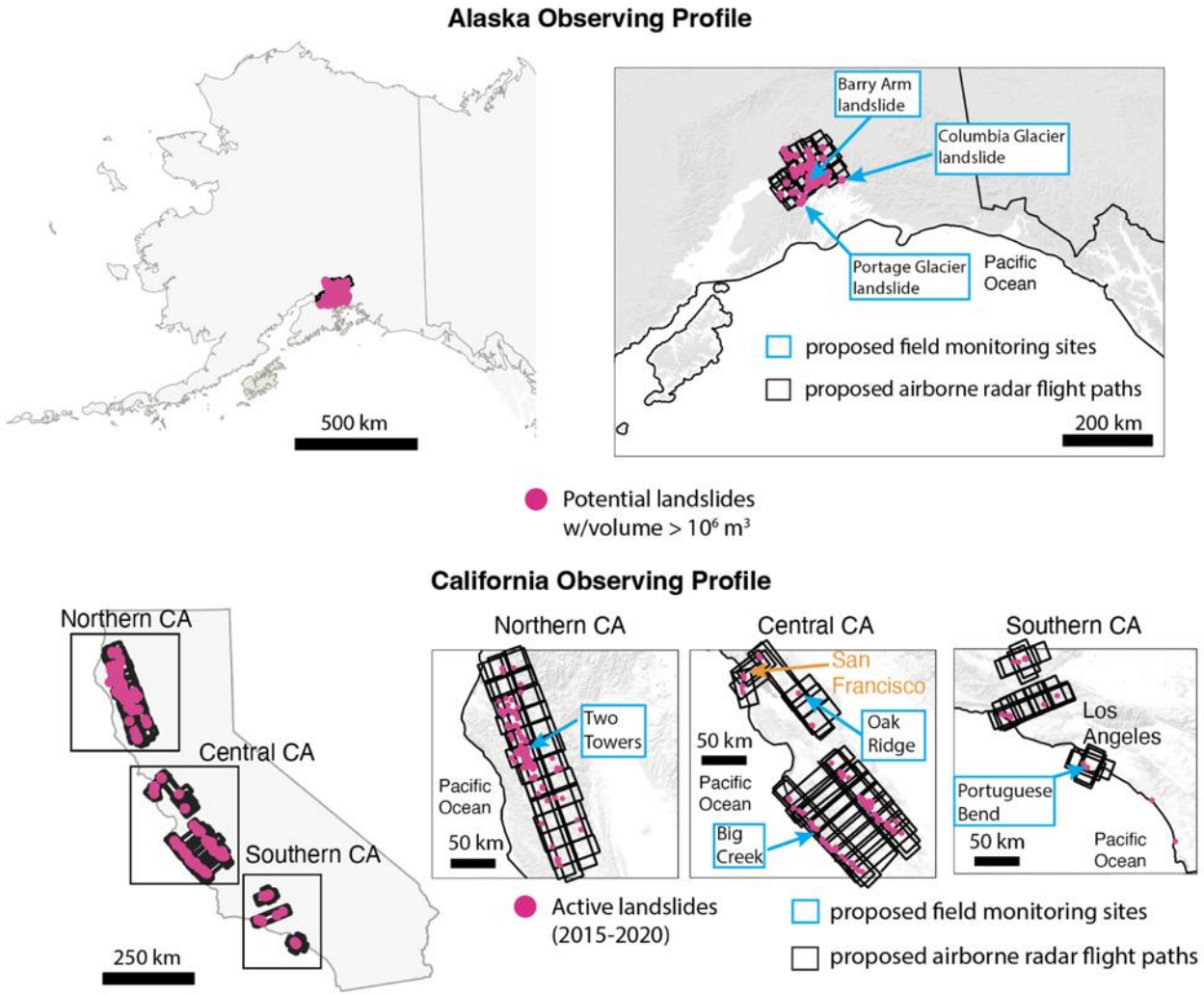

Fig. 8. Alaska and California observing profile showing flight paths and proposed/potential field monitoring sites. Note again that the "Potential landslides" shown in Alaska are locations that show signs of instability but there are little to no kinematic measurements for confirmation. The "Active landslides" in California are locations of confirmed movement from moderate resolution satellite InSAR [23]. In both cases, locations are used to target areas with potentially high landslide density.

A1 Appendix 1: Science Measurement Requirement and Science Modeling Requirements Matrices

A1.1.1 Science Measurement Requirement Matrix

Table A1.1.1-1. Science Measurement Requirement Matrix. Airborne measurements in blue text, ground measurements in green text.

Scientific Measurement Requirement			Science Question & Objective Addressed	Threshold (T) or Baseline (B)	Priority Rating*
Observables	Technique/Instrument/ Method	Required Value			
3D ground surface displacement	• Repeat-pass InSAR (L- and P-band) along 3 or more overlapping flight paths in landslide areas; • Repeat-pass pixel offset tracking with SAR and optical imagery (Baseline); • GPS and extensometers at select landslide sites	• Accuracy: < 1 cm, • Precision: < 1 cm, • Resolution: ≤ 10 m, • Accuracy: < 5 mm, • Precision: < 5 mm, • Resolution: point	[Q1 O1], [Q1 O2], [Q2 O3], [Q2 O4]	T and B	1
Subsurface landslide geometry	Borehole inclinometer at selected sites in CA	• Accuracy: 1 cm, • Horizontal Resolution: point measure; • Vertical Resolution: 10 cm	[Q1 O1], [Q1 O2]	T	1
	Seismic velocity (geophones to measure P- and S-wave arrivals) along multiple transects at selected sites in CA and AK	Accuracy: 0.20 µV, RFI at 2 ms, 36 dB, 1.75 to 208 Hz, • Vertical Resolution: shallow (top 2 m: 0.25 m; 2 – 10 m depth: 1 m; below 10 m: > 2 m), • Horizontal resolution: 1 m	[Q1 O1], [Q1 O2], [Q2 O3], [Q2 O4]	T and B	3
Ground surface elevation	Stereo optical imagery (Baseline).	• Accuracy: < 0.5 m, • Precision: < 0.5 m, • Resolution: ≤ 5 m,	[Q1 O1], [Q2 O3], [Q2 O4]	T and B	2
Soil moisture	Single-pass quad-pol SAR (L- and P-band) along 3 or more overlapping flight paths in landslide areas. Soil moisture sensors at selected sites in CA and AK	• Accuracy: < 0.1 m^3/m^3, • Precision: < 0.1 m^3/m^3, • Resolution: ≤ 10 m, • Accuracy: <0.04 m^3/m^3 • Resolution: point measure at depths of 5, 10, 25, 50, 100, 200 cm	[Q1 O2]	T and B	1

Pore-water Pressure	Grouted borehole piezometers at select landslide sites in CA	• Accuracy range: 0.08 - 70 kPa; • Precision: 0.0175 kPa; • Resolution: point measure at 4 depths (shallow and deep relative to base of landslide)	[Q1 O2]	T	1
Precipitation	Rain gauge at select landslide sites in CA	• Accuracy: 0.1 mm, • Resolution: point measure	[Q1 O2]	T	2
Ground water content	Electrical resistivity at select landslide sites in CA	• Accuracy: 1 Ω-m, • Resolution: 5 m, • Accuracy: 100 dB at >20 Hz. • Resolution: < 1 m at < 2 m depth, > 1 m between 2 and 5 m depth, may not have sufficient resolution below 10 m depth.	[Q1 O2]	T	3
Landslide hydraulic properties	Guelph Permeameter in boreholes in CA; slug tests, and laboratory analyses	• Accuracy range: 10^{-10} to 10^{-2} m/s • Resolution: point measure	[Q2 O2]	T	1
Landslide frictional strength	**Lab**: rotary or direct shear measurement	**Lab:** Accuracy: 1 kPa • Resolution: N/A	[Q1 O1], [Q1 O2], [Q2 O3], [Q2 O4]	T and B	1

* 1 = required, 2 = desired, 3 = useful

A1.1.2 Science Modeling Requirement Matrix

Based on our Science Objectives, we have identified the following Scientific Modeling Capabilities and derived the measurement requirements to feed the models in Table A1.1.2-1 Science Modeling Requirement Matrix.

Table A1.1.2-1. Science Modeling Requirement Matrix

Scientific Modeling Capability	Scientific Measurement Requirement (for the model)			Science Question & Objective Addressed	Threshold (T) or Baseline (B)	Priority Rating*
	Physical Parameters	Observables	Required Value			
Subsurface Landslide Geometry Inversion	• 3D ground surface displacement; • Ground surface elevation; • Subsurface landslide geometry	Table A1.1.1-1		[Q1 O1], [Q1 O2], [Q2 O3], [Q2 O4]	T and B	1
Soil moisture depth profile estimation model	• Soil moisture; • Precipitation	Table A1.1.1-1		[Q1 O2]	T	1
Groundwater flow model	• Soil Moisture; • Pore-water pressure; • Precipitation;	Table A1.1.1-1		[Q1 O2]	T	1

	• Hydraulic properties; • Electrical resistivity for groundwater content				
Shallow seismic velocity inversion model	• Seismic velocity (geophones) along multiple transects at selected sites	Table A1.1.1-1	[Q1 O1], [Q1 O2], [Q2 O3], [Q2 O4]	T and B	2
Electrical Resistivity tomography model	• Electrical resistivity at select landslide sites	Table A1.1.1-1	[Q1 O1], [Q1 O2], [Q2 O3]	T and B	3
Landslide mechanical-hydrological model	• 3D ground surface displacement; • Ground surface elevation; • Subsurface landslide geometry; • Soil moisture; • Pore-water pressure; • Precipitation; • Mechanical properties; • Hydraulic properties	Table A1.1.1-1	[Q1 O1], [Q1 O2], [Q2 O3], [Q2 O4	T and B	1

* 1 = required, 2 = desired, 3 = useful

Acknowledgements

Part of this research was carried out at the Jet Propulsion Laboratory, California Institute of Technology, under a contract with the National Aeronautics and Space Administration (80NM0018D0004).

A2 Appendix 2: References

[1] R. M. Iverson *et al.*, "Landslide mobility and hazards: Implications of the 2014 Oso disaster," *Earth and Planetary Science Letters*, vol. 412, pp. 197–208, 2015.

[2] N. Nappo, D. Peduto, O. Mavrouli, C. J. van Westen, and G. Gullà, "Slow-moving landslides interacting with the road network: Analysis of damage using ancillary data, in situ surveys and multi-source monitoring data," *Engineering geology*, vol. 260, p. 105244, 2019.

[3] B. H. Mackey and J. J. Roering, "Sediment yield, spatial characteristics, and the long-term evolution of active earthflows determined from airborne LiDAR and historical aerial photographs, Eel River, California," *Geological Society of America Bulletin*, vol. 123, no. 7–8, pp. 1560–1576, 2011.

[4] R. L. Schuster and L. Highland, *Socioeconomic and environmental impacts of landslides in the western hemisphere*. Citeseer, 2001.

[5] D. Kirschbaum, T. Stanley, and Y. Zhou, "Spatial and temporal analysis of a global landslide catalog," *Geomorphology*, vol. 249, pp. 4–15, 2015.

[6] M. J. Froude and D. Petley, "Global fatal landslide occurrence from 2004 to 2016," *Natural Hazards and Earth System Sciences*, vol. 18, pp. 2161–2181, 2018.

[7] N. Oreskes, "Landslides Kill and Hurt Thousands, but Science Largely Ignores These Disasters," Apr. 01, 2023. [Online]. Available: https://www.scientificamerican.com/article/landslides-kill-and-hurt-thousands-but-science-largely-ignores-these-disasters/

[8] M. J. Crozier, "Deciphering the effect of climate change on landslide activity: A review," *Geomorphology*, vol. 124, no. 3–4, pp. 260–267, 2010.

[9] S. L. Gariano and F. Guzzetti, "Landslides in a changing climate," *Earth-Science Reviews*, vol. 162, pp. 227–252, 2016.

[10] A. I. Patton, S. L. Rathburn, and D. M. Capps, "Landslide response to climate change in permafrost regions," *Geomorphology*, vol. 340, pp. 116–128, 2019.

[11] P. Lacroix, A. L. Handwerger, and G. Bièvre, "Life and death of slow-moving landslides," *Nature Reviews Earth & Environment*, pp. 1–16, 2020.

[12] A. L. Handwerger, M.-H. Huang, E. J. Fielding, A. M. Booth, and R. Bürgmann, "A shift from drought to extreme rainfall drives a stable landslide to catastrophic failure," *Scientific Reports*, vol. 9, no. 1, p. 1569, Feb. 2019, doi: 10.1038/s41598-018-38300-0.

[13] E. Intrieri *et al.*, "The Maoxian landslide as seen from space: detecting precursors of failure with Sentinel-1 data," *Landslides*, vol. 15, pp. 123–133, 2018.

[14] P. Lacroix, J. Huanca, L. Albinez, and E. Taipe, "Precursory Motion and Time-Of-Failure Prediction of the Achoma Landslide, Peru, From High Frequency PlanetScope Satellites," *Geophysical Research Letters*, vol. 50, no. 19, p. e2023GL105413, 2023.

[15] X. Li, A. L. Handwerger, G. Peltzer, and E. Fielding, "Exploring the behaviors of initiated progressive failure and slow-moving landslides in Los Angeles using satellite InSAR and pixel offset tracking," *Geophysical Research Letters*, vol. 51, no. 13, p. e2024GL108267, 2024.

[16] N. J. Finnegan, E. E. Brodsky, H. M. Savage, A. L. Nereson, and C. R. Murphy, "Seasonal Slow Landslide Displacement Is Accommodated by mm-Scale Stick-Slip Events," *Geophysical Research Letters*, vol. 49, no. 20, p. e2022GL099548, 2022.

[17] F. K. Rengers, L. A. McGuire, J. W. Kean, D. M. Staley, and D. E. J. Hobley, "Model simulations of flood and debris flow timing in steep catchments after wildfire," *Water Resources Research*, vol. 52, no. 8, pp. 6041–6061, 2016.

[18] D. L. Swain, B. Langenbrunner, J. D. Neelin, and A. Hall, "Increasing precipitation volatility in twenty-first-century California," *Nature Climate Change*, p. 1, 2018.

[19] J. D. Shakun, P. U. Clark, F. He, N. A. Lifton, Z. Liu, and B. L. Otto-Bliesner, "Regional and global forcing of glacier retreat during the last deglaciation," *Nature Communications*, vol. 6, no. 1, p. 8059, 2015.

[20] C. Sommer, P. Malz, T. C. Seehaus, S. Lippl, M. Zemp, and M. H. Braun, "Rapid glacier retreat and downwasting throughout the European Alps in the early 21st century," *Nature communications*, vol. 11, no. 1, p. 3209, 2020.
[21] C. Dai *et al.*, "Detection and assessment of a large and potentially tsunamigenic periglacial landslide in Barry Arm, Alaska," *Geophysical research letters*, vol. 47, no. 22, p. e2020GL089800, 2020.
[22] P. Lacroix, J. M. Belart, E. Berthier, Þ. Sæmundsson, and K. Jónsdóttir, "Mechanisms of landslide destabilization induced by glacier-retreat on Tungnakvíslarjökull area, Iceland," *Geophysical Research Letters*, vol. 49, no. 14, p. e2022GL098302, 2022.
[23] A. L. Handwerger, E. J. Fielding, S. S. Sangha, and D. P. Bekaert, "Landslide sensitivity and response to precipitation changes in wet and dry climates," *Geophysical research letters*, vol. 49, no. 13, p. e2022GL099499, 2022.
[24] C. R. Murphy, N. J. Finnegan, and F. K. J. Oberle, "Vadose zone thickness limits pore-fluid pressure rise in a large, slow-moving earthflow," *Journal of Geophysical Research: Earth Surface*, vol. 127, no. 6, p. e2021JF006415, 2022.
[25] G. G. Persad, D. L. Swain, C. Kouba, and J. P. Ortiz-Partida, "Inter-model agreement on projected shifts in California hydroclimate characteristics critical to water management," *Climatic Change*, vol. 162, no. 3, pp. 1493–1513, 2020.
[26] J. A. Warrick, A. C. Ritchie, K. M. Schmidt, M. E. Reid, and J. Logan, "Characterizing the catastrophic 2017 Mud Creek landslide, California, using repeat structure-from-motion (SfM) photogrammetry," *Landslides*, pp. 1–19, 2019.
[27] D. L. Swain, "A shorter, sharper rainy season amplifies California wildfire risk," *Geophysical Research Letters*, vol. 48, no. 5, p. e2021GL092843, 2021.
[28] G. L. Bennett, J. J. Roering, B. H. Mackey, A. L. Handwerger, D. A. Schmidt, and B. P. Guillod, "Historic drought puts the brakes on earthflows in Northern California," *Geophysical Research Letters*, vol. 43, no. 11, pp. 5725–5731, 2016.
[29] A. L. Handwerger, E. J. Fielding, M.-H. Huang, G. L. Bennett, C. Liang, and W. H. Schulz, "Widespread initiation, reactivation, and acceleration of landslides in the northern California Coast Ranges due to extreme rainfall," *Journal of Geophysical Research: Earth Surface*, vol. 124, no. 7, pp. 1782–1797, 2019.
[30] N. J. Finnegan, J. P. Perkins, A. L. Nereson, and A. L. Handwerger, "Unsaturated Flow Processes and the Onset of Seasonal Deformation in Slow-Moving Landslides," *Journal of Geophysical Research: Earth Surface*, vol. 126, no. 5, p. e2020JF005758, 2021.
[31] C. F. Larsen, R. J. Motyka, A. A. Arendt, K. A. Echelmeyer, and P. E. Geissler, "Glacier changes in southeast Alaska and northwest British Columbia and contribution to sea level rise," *Journal of Geophysical Research: Earth Surface*, vol. 112, no. F1, 2007.
[32] C. F. Larsen, E. Burgess, A. A. Arendt, S. O'neel, A. J. Johnson, and C. Kienholz, "Surface melt dominates Alaska glacier mass balance," *Geophysical Research Letters*, vol. 42, no. 14, pp. 5902–5908, 2015.
[33] H.-O. Pörtner *et al.*, *Climate change 2022: Impacts, adaptation and vulnerability*. IPCC Geneva, Switzerland:, 2022.
[34] B. M. Higman *et al.*, "100 Giant Alaska Landslides," in *Fall Meeting 2022*, AGU, 2022.
[35] J. Kim, J. A. Coe, Z. Lu, N. N. Avdievitch, and C. P. Hults, "Spaceborne InSAR mapping of landslides and subsidence in rapidly deglaciating terrain, Glacier Bay National Park and Preserve and vicinity, Alaska and British Columbia," *Remote Sensing of Environment*, vol. 281, p. 113231, 2022.
[36] L. N. Schaefer, J. Kim, D. M. Staley, Z. Lu, and K. R. Barnhart, "Satellite Interferometry Landslide Detection and Preliminary Tsunamigenic Plausibility Assessment in Prince William Sound, Southcentral Alaska," US Geological Survey, 2024.
[37] K. R. Barnhart, R. P. Jones, D. L. George, J. A. Coe, and D. M. Staley, "Preliminary assessment of the wave generating potential from landslides at Barry Arm, Prince William Sound, Alaska," US Geological Survey, 2021.
[38] D. J. Miller, "The Alaska earthquake of July 10, 1958: giant wave in Lituya Bay," *Bulletin of the Seismological Society of America*, vol. 50, no. 2, pp. 253–266, 1960.
[39] G. C. Wiles and P. E. Calkin, "Reconstruction of a debris-slide-initiated flood in the southern Kenai Mountains, Alaska," *Geomorphology*, vol. 5, no. 6, pp. 535–546, 1992.

[40] B. Higman *et al.*, "The 2015 landslide and tsunami in Taan Fiord, Alaska," *Scientific reports*, vol. 8, no. 1, p. 12993, 2018.
[41] Resource Development Council for Alaska, Inc, "RDC request for a temporary wavier to the Passenger Vessel Services Act," Mar. 17, 2020. [Online]. Available: https://www.akrdc.org/requestpvsawaiver
[42] M. C. Strzelecki and M. W. Jaskólski, "Arctic tsunamis threaten coastal landscapes and communities–survey of Karrat Isfjord 2017 tsunami effects in Nuugaatsiaq, western Greenland," *Natural Hazards and Earth System Sciences*, vol. 20, no. 9, pp. 2521–2534, 2020.
[43] M. Geertsema *et al.*, "The 28 November 2020 landslide, tsunami, and outburst flood–A hazard cascade associated with rapid deglaciation at Elliot Creek, British Columbia, Canada," *Geophysical research letters*, vol. 49, no. 6, p. e2021GL096716, 2022.
[44] J. A. Coe, "Landslide hazards and climate change: A perspective from the United States," in *Slope safety preparedness for impact of climate change*, CRC Press, 2017, pp. 479–523.
[45] A. E. East and J. B. Sankey, "Geomorphic and sedimentary effects of modern climate change: current and anticipated future conditions in the western United States," *Reviews of Geophysics*, vol. 58, no. 4, p. e2019RG000692, 2020.
[46] B. Bayer, A. Simoni, M. Mulas, A. Corsini, and D. Schmidt, "Deformation responses of slow moving landslides to seasonal rainfall in the Northern Apennines, measured by InSAR," *Geomorphology*, vol. 308, pp. 293–306, 2018.
[47] Y. Xu, W. H. Schulz, Z. Lu, J. Kim, and K. Baxtrom, "Geologic controls of slow-moving landslides near the US West Coast," *Landslides*, pp. 1–13, 2021.
[48] A. L. Handwerger, A. M. Booth, M.-H. Huang, and E. J. Fielding, "Inferring the Subsurface Geometry and Strength of Slow-Moving Landslides Using 3-D Velocity Measurements From the NASA/JPL UAVSAR," *Journal of Geophysical Research: Earth Surface*, vol. 126, no. 3, p. e2020JF005898, 2021.
[49] A. M. Booth, J. C. McCarley, and J. Nelson, "Multi-year, three-dimensional landslide surface deformation from repeat lidar and response to precipitation: Mill Gulch earthflow, California," *Landslides*, pp. 1–14, 2020.
[50] T.-H. Liao, S.-B. Kim, A. L. Handwerger, and E. J. Fielding, "Soil Moisture Retrieval Using L-Band SAR Over Landslide Regions in Northern California Grasslands," in *2021 IEEE International Geoscience and Remote Sensing Symposium IGARSS*, IEEE, 2021, pp. 5881–5883.
[51] R. W. Healy, *Simulation of Solute Transport Invariably Saturated Porous Media with Supplemental Information on Modifications to the US Geological Survey's Computer Program VS2D*, vol. 90, no. 4025. Department of the Interior, US Geological Survey, 1990.
[52] E. G. Lappala, R. W. Healy, and E. P. Weeks, *Documentation of computer program VS2D to solve the equations of fluid flow in variably saturated porous media*, vol. 83, no. 4099. Department of the Interior, US Geological Survey, 1987.
[53] C. Lanni, J. McDonnell, L. Hopp, and R. Rigon, "Simulated effect of soil depth and bedrock topography on near-surface hydrologic response and slope stability," *Earth surface processes and landforms*, vol. 38, no. 2, pp. 146–159, 2013.
[54] W. H. Schulz, J. B. Smith, G. Wang, Y. Jiang, and J. J. Roering, "Clayey landslide initiation and acceleration strongly modulated by soil swelling," *Geophysical Research Letters*, vol. 45, no. 4, pp. 1888–1896, 2018.
[55] J. S. Whiteley *et al.*, "Rapid characterisation of landslide heterogeneity using unsupervised classification of electrical resistivity and seismic refraction surveys," *Engineering Geology*, vol. 290, p. 106189, 2021.
[56] M. E. Reid, S. B. Christian, D. L. Brien, and S. Henderson, "Scoops3D–software to analyze three-dimensional slope stability throughout a digital landscape," *US Geological Survey Techniques and Methods, book*, vol. 14, 2015.
[57] R. M. Iverson, "Regulation of landslide motion by dilatancy and pore pressure feedback," *Journal of Geophysical Research: Earth Surface*, vol. 110, no. F2, 2005.
[58] A. L. Handwerger, A. W. Rempel, R. M. Skarbek, J. J. Roering, and G. E. Hilley, "Rate-weakening friction characterizes both slow sliding and catastrophic failure of landslides," *Proceedings of the National Academy of Sciences*, vol. 113, no. 37, pp. 10281–10286, 2016.
[59] E. E. Alonso, "Triggering and motion of landslides," *Géotechnique*, vol. 71, no. 1, pp. 3–59, 2021.

[60] N. J. Finnegan and D. M. Saffer, "Seasonal slow slip in landslides as a window into the frictional rheology of creeping shear zones," *Science Advances*, vol. 10, no. 42, p. eadq9399, 2024.
[61] T. W. Lambe and R. V. Whitman, "Soil mechanics, Series in soil engineering," *Jhon Wiley & Sons*, 1969.
[62] S. T. McColl and T. R. Davies, "Large ice-contact slope movements: Glacial buttressing, deformation and erosion," *Earth Surface Processes and Landforms*, vol. 38, no. 10, pp. 1102–1115, 2013.